Polymer 50 (2009) 1054–1061

Contents lists available at ScienceDirect

Polymer

journal homepage: www.elsevier.com/locate/polymer

Structural effects of ionomers on the morphology, isothermal crystallization kinetics and melting behaviors of PET/ionomers

Shidong Tang, Zhong Xin*

State Key Laboratory of Chemical Engineering, East China University of Science and Technology, Shanghai 200237, China

ARTICLE INFO

Article history:
Received 16 July 2008
Received in revised form
12 November 2008
Accepted 8 December 2008
Available online 11 December 2008

Keywords:
Morphology
Ionomer
PET

ABSTRACT

Morphology, isothermal crystallization kinetics and melting behaviors of PET modified by low molecular weight of ionomers with different structures, ethylene–sodium acrylate (AClyn) and styrene–sodium acrylate (SAA–Na), have been investigated by scanning electron microscopy (SEM), differential scanning calorimeter (DSC) and polarizing optical microscopy (POM). At both high and low temperature regions, AClyn and SAA–Na act as heterogeneous nucleating agent to induce the formation of PET nuclei. The presence of benzene side group in SAA–Na increased the interactions between PET and SAA–Na, leading better compatibility of PET/SAA–Na than that of PET/AClyn. Although SAA–Na had less sodium ions than AClyn at the same content, SAA–Na exhibited similar efficiency to enhance the crystallization rate of PET with AClyn. Isothermal kinetic analysis showed that the same growth dimension was obtained for PET/ionomers regardless of the structural difference between AClyn and SAA–Na. After isothermal melt-crystallization, the second peak of multiple melting endotherms of PET/SAA–Na had almost the same value with PET/AClyn.

1. Introduction

Poly(ethylene terephthalate) (PET) has been widely used as industrial films and engineering plastics because of its excellent physical properties. However, PET exhibits a rather slow crystallization rate, which limits its application in engineering plastics. Inorganic substances [1–3] and organic salts especially the alkali metal salts of aromatic carboxylic acid [4–6] have been used as nucleating agent to enhance the crystallization rate of PET.

Ionomers are polymeric materials having a small number of ionic side groups in the hydrophobic backbone chains, which cause slight molecular weight reduction of PET and have been commercially recognized as the most effective nucleating agents for PET [7]. Ethylene-based ionomers [8–13], ionic-ended polyesters [14] or styrene-based ionomers [15] have been reported as nucleating agent in PET. In PET/PE blends, the addition of ionomer can improve both the compatibility and crystallization of blends [16–21]. Yu et al. [8] reported that the ionomer ethylene–sodium acrylate (trade name AClyn) was more effective than ethylene–sodium methacrylate (trade name Surlyn) to enhance the crystallization rate of PET because of their different nucleation mechanism. Their further investigations indicated that the nucleation efficiency of ionomers based on ethylene–acrylic acid depends on the nature of cation [9]. From our previous work, it was found that the styrene–sodium acrylate ionomers initiated heterogeneous nucleation and their chemical structure determined the aggregation behaviors of ionomers, which affected the crystallization behaviors of PET/ionomer.

To further disclose the relationship between the structure of ionomer and the crystallization properties of PET/ionomer, ethylene–sodium acrylate ionomer (AClyn) and styrene–sodium acrylate ionomer (SAA–Na) with the similar molecular weight and mole fraction of sodium acrylate, were mixed with PET. The morphology, isothermal crystallization kinetics and melting behaviors of PET/ionomers were investigated.

2. Experimental

2.1. Materials

Poly(ethylene terephthalate) with intrinsic viscosity of 0.68 dL/g in phenol/tetrachloroethane mixture (1:1 by weight) was kindly supplied by Sinopec Yizheng Chemical Fibre Company Limited (YCF), China. The ionomer styrene–sodium acrylate (SAA–Na) was obtained by 100% neutralization of the styrene–acrylic acid copolymer, which was prepared by copolymerization in benzene solution with azodiisobutyronitrile (AIBN) as initiator [22] and had molecular weight (M_w) of 2.3×10^3 and 9.2 mol% of acrylic acid. AClyn was received from HoneyWell (China) Co. Ltd, which was

* Corresponding author. Tel.: +86 21 64252972; fax: +86 21 64240862.
E-mail address: xzh@ecust.edu.cn (Z. Xin).

0032-3861/$ – see front matter © 2008 Elsevier Ltd. All rights reserved.
doi:10.1016/j.polymer.2008.12.015

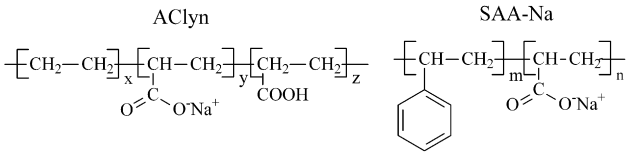

Fig. 1. Structure of AClyn and SAA–Na.

a 80 wt% sodium neutralized ethylene–acrylic acid copolymer (80/20 by weight, 93.5/6.5 by mole, and $M_w < 3000$) in the form of pellets [23]. Fig. 1 shows the chemical structure of AClyn and SAA–Na.

Table 1
Sample code, ionomer and content of ionomer.

Sample	Ionomer	Content of ionomer (wt%)
PET	None	0
S01	SAA–Na	0.1
S05	SAA–Na	0.5
S10	SAA–Na	1.0
S20	SAA–Na	2.0
S50	SAA–Na	5.0
A01	AClyn	0.1
A05	AClyn	0.5
A10	AClyn	1.0
A20	AClyn	2.0
A50	AClyn	5.0

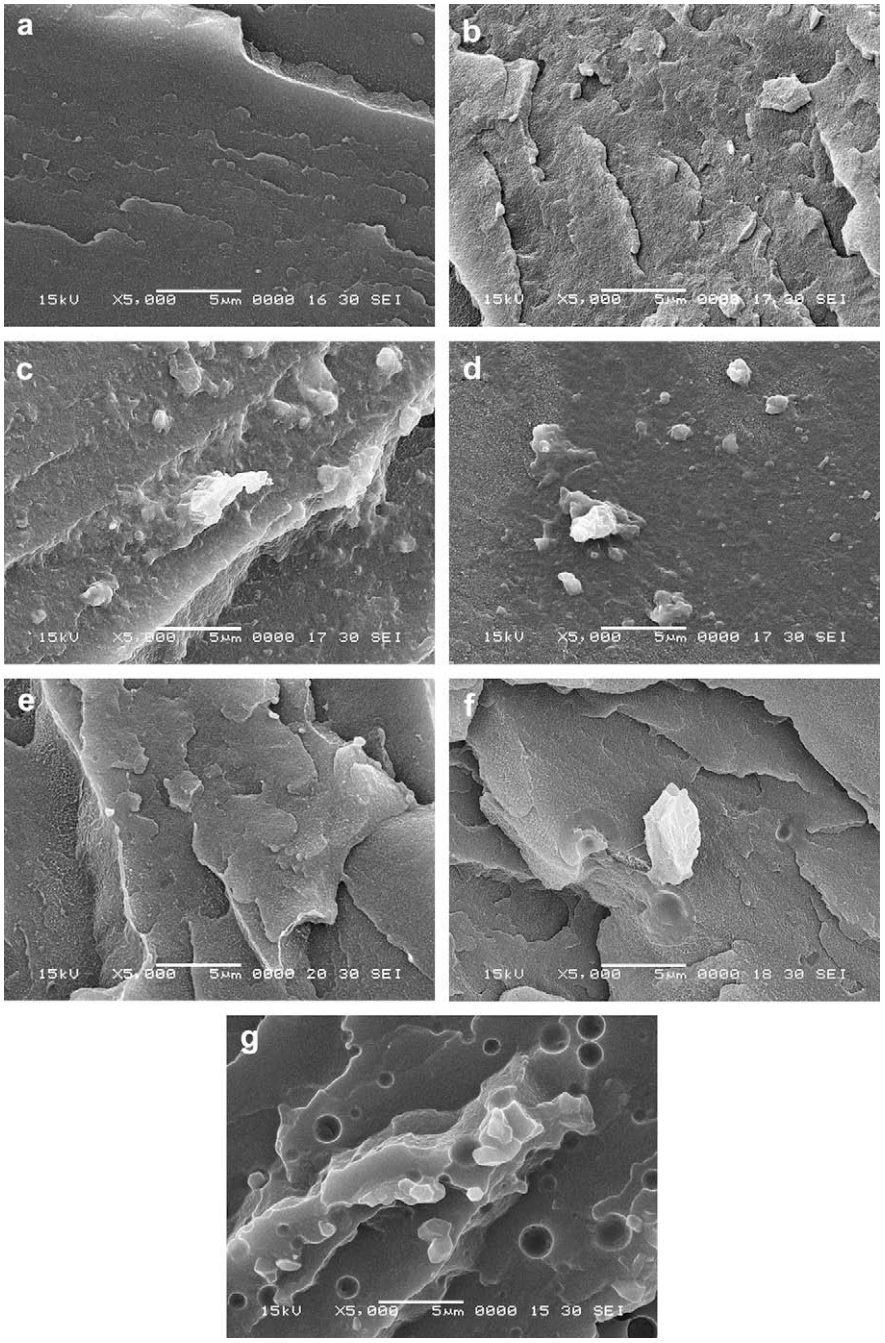

Fig. 2. SEM micrographs of (a) PET, (b) S01, (c) S10, (d) S50, (e) A01, (f) A10, (g) A50.

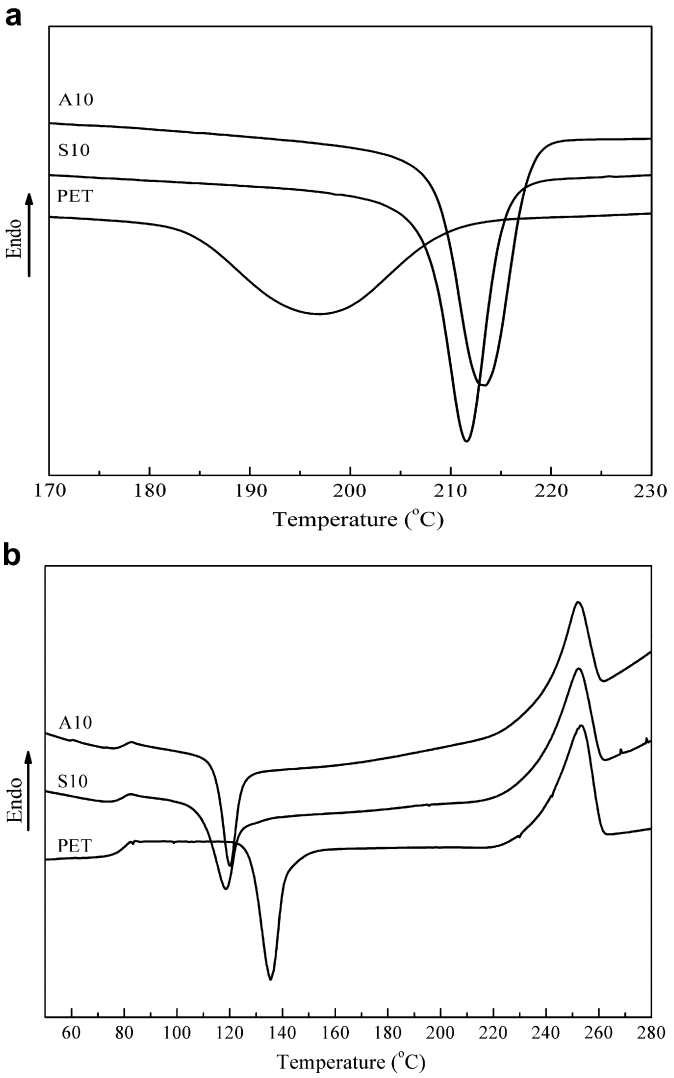

Fig. 3. DSC curves of (a) melt-crystallization, (b) cold-crystallization for neat PET, S10 and A10.

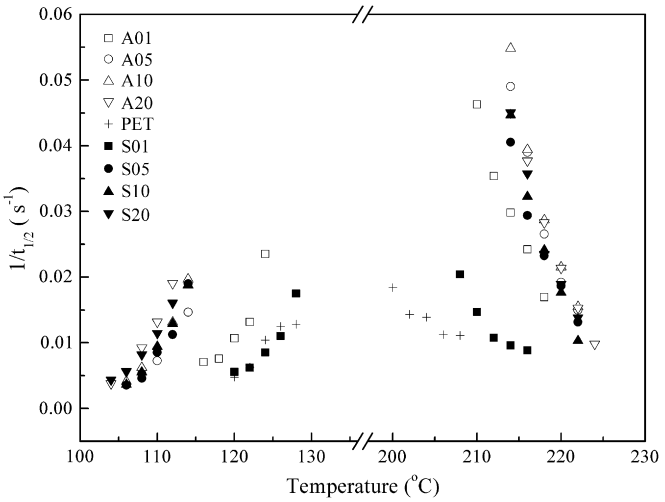

Fig. 5. Overall crystallization rate of various PET samples as a function of the crystallization temperature (T_c).

2.2. Preparation of PET/ionomers [8]

Before use, PET was dried at 120 °C for 24 h, SAA–Na and AClyn were dried at 70 °C for 12 h under vacuum. PET was mixed with SAA–Na or AClyn in a self-designed flask, which had an inlet and outlet for nitrogen. After removing air with nitrogen for 10 min, the temperature was raised to about 270 °C and held for 5 min to achieve equilibrium. At this temperature the mixture was stirred for 5 min and then collected for measurement. The neat PET was also subjected to the same procedure. Corresponding to the type and content of ionomer, samples were named as neat PET, S series and A series, as shown in Table 1.

2.3. Measurement

The thermal behavior of ionomer was measured by using TGA (SDT Q600, TA Instruments). The samples of about 10 mg were heated from room temperature to 600 °C at 10 °C/min in a nitrogen atmosphere.

The morphology of PET sample was investigated by Scanning Electron Microscopy (SEM) (JEOL JSM-6360LV, Japan).

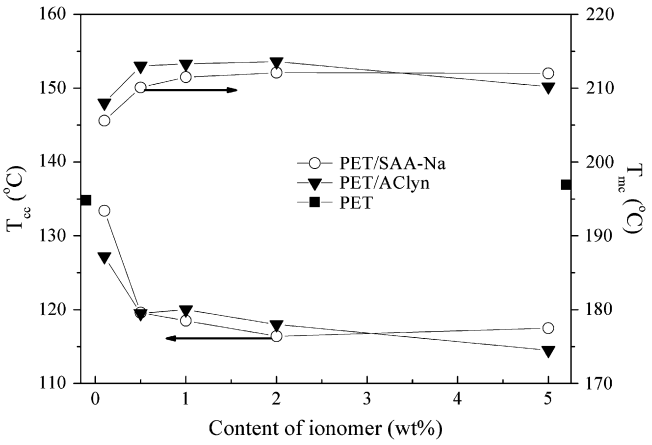

Fig. 4. Relationship between the content of ionomers and the crystallization of PET.

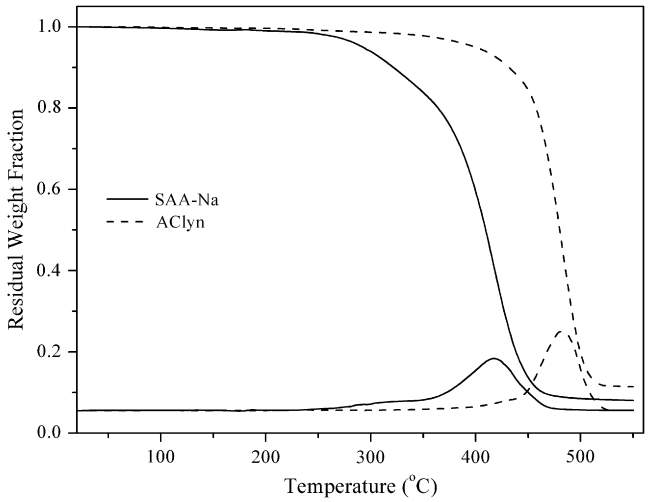

Fig. 6. TGA and DTG curves of ionomer SAA–Na and AClyn.

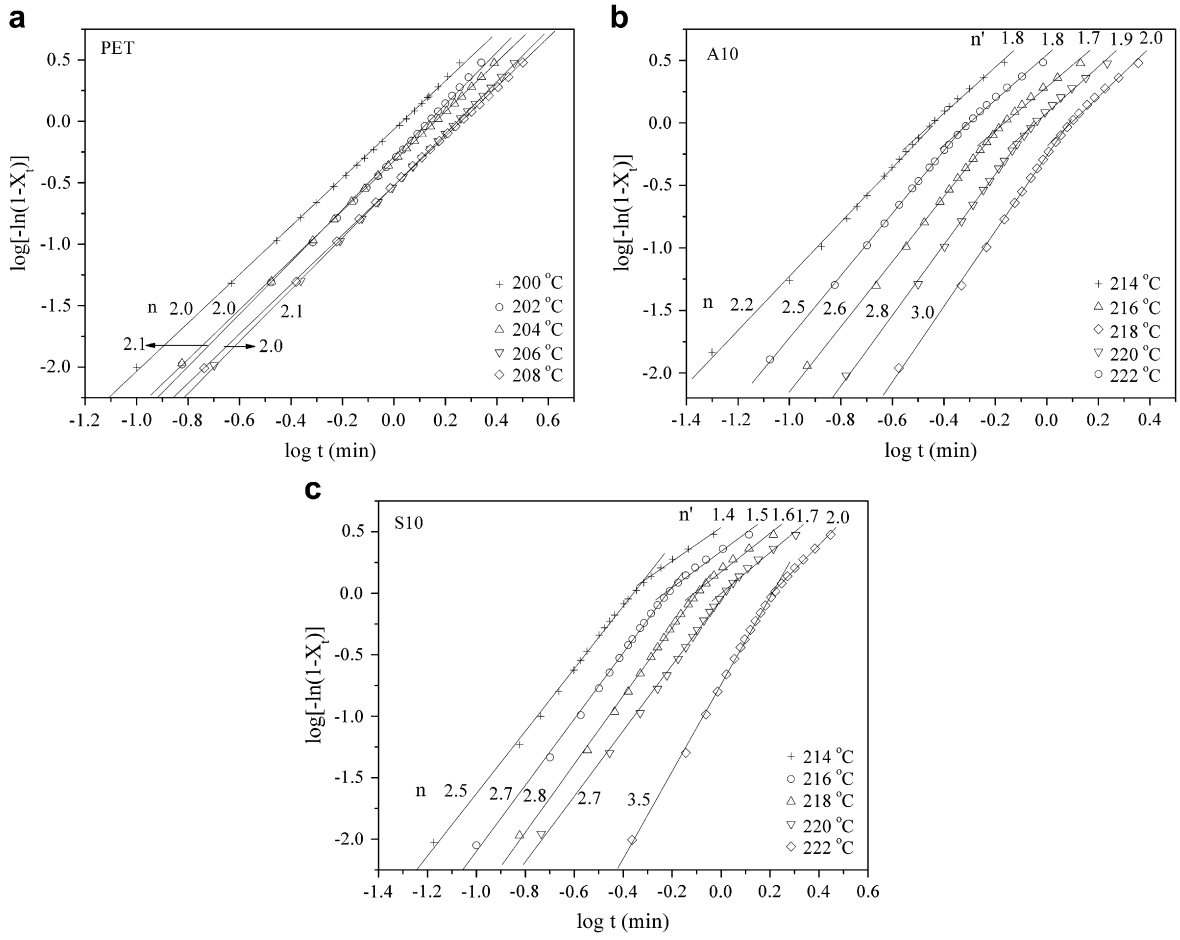

Fig. 7. Avrami plots of (a) PET, (b) A10, (c) S10 for isothermal melt-crystallization.

The sample was free-fractured and coated with gold to enhance conductivity.

The crystallization of PET sample was measured with Differential Scanning Calorimeter (DSC) (Diamond, PerkinElmer) in a nitrogen atmosphere. Calibration was conducted with standard indium. The sample with weight of 3–4 mg was first melted at 300 °C for 5 min, then quenched to liquid nitrogen, resulting in amorphous PET sample. The quenched sample was heated in DSC cell from 0 °C to 300 °C at 10 °C/min. From this DSC curve we can get cold-crystallization temperature (T_{cc}). To study the melt-crystallization temperature (T_{mc}), PET sample was directly melted in DSC cell at 300 °C for 5 min to remove thermal history and cooled at 10 °C/min to 50 °C. From the cooling curve we can get T_{mc}.

Isothermal cold-crystallization studies were done by heating the quenched samples from 50 °C to the selected crystallization temperature at a heating rate of 100 °C/min. They were kept at the crystallization temperature for sufficient time so that the DSC trace returned to the calorimeter baseline. To investigate the isothermal melt-crystallization and melting behaviors, the samples were heated to 300 °C quickly, held for 5 min, then cooled to the selected crystallization temperature at a rate of 100 °C/min and kept at that temperature until the DSC trace returned to the calorimeter baseline. At last the samples were heated immediately to 300 °C at a rate of 10 °C/min. The fractional crystallinity X_t, which developed at time t, was

$$X_t = \frac{\int_0^t (\mathrm{d}H_c/\mathrm{d}t)\mathrm{d}t}{\int_0^\infty (\mathrm{d}H_c/\mathrm{d}t)\mathrm{d}t}$$

where $\mathrm{d}H_c/\mathrm{d}t$ is the heat flow rate, $\int_0^\infty (\mathrm{d}H_c/\mathrm{d}t)\mathrm{d}t$ is the total area under the crystallization exotherm at the crystallization temperature.

Optical micrographs were obtained with polarizing optical microscopy (POM) (BX51, Olympus). A thin sample piece was sandwiched between two glass coverslips and placed on the digital hotplate under nitrogen. The hotplate was rapidly heated to 300 °C and kept for 5 min, the melt was gently pressed to achieve a uniform thickness, then cooled to 220 °C at a rate of 100 °C/min, images were recorded by the CCD camera.

3. Results and discussion

3.1. Morphology of PET/ionomers

The fractured surfaces of PET modified by the styrene–sodium acrylate ionomer (SAA–Na) and ethylene–sodium acrylate ionomer (AClyn) are shown in Fig. 2. In PET/SAA–Na, only white specks existed on the PET matrix surface (Fig. 2(c)), and this feature was more obvious with increasing the content of SAA–Na ((d)). Comparing with the surface of neat PET (Fig. 2(a)), it can be seen that the white specks should be the ionomer SAA–Na, which during the fracture elongated more than PET but was not pulled out. However, SEM micrographs of PET/AClyn (Fig. 2(e)–(g)) showed that besides the white particles of AClyn, there were voids with smooth surfaces and their shapes were very different from the particles. The T_m of AClyn is 85 °C [23], which is

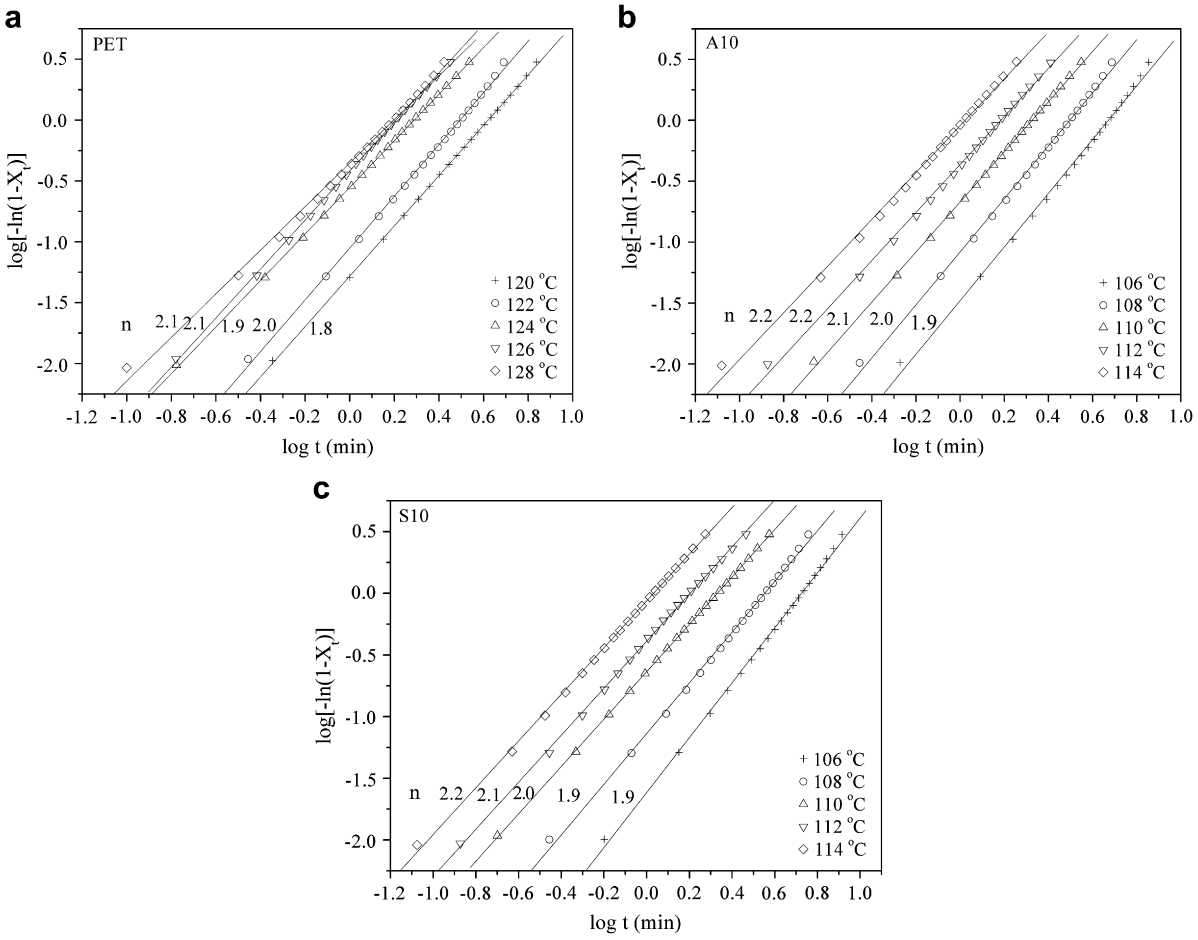

Fig. 8. Avrami plots of (a) PET, (b) A10, (c) S10 for isothermal cold-crystallization.

extremely lower than the crystallization temperature of PET from the melt, thus the melt of AClyn could separate from the solid PET phase (the formation of voids) after the crystallization of PET and then crystallize to form particles. These results indicated that the compatibility between PET and SAA–Na was better than that of PET/AClyn.

The compatibility between PET and ionomer is due to the ion–dipole interactions between the acid in ionomer and the carbonyl groups of PET [24]. On the other hand, the interactions between molecules of ionomer result in the aggregation of sodium ions in ionomer [25], which would decrease the interactions between PET and ionomer. The two interactions are influenced by many factors, such as chemical structure. Suchocka-Gałas [25] has reported that the interactions between molecules of styrene–sodium methacrylate ionomer were weaker than that of styrene–sodium acrylate ionomer due to the presence of methyl group on the α-carbon. In this paper, AClyn and SAA–Na both are ethylene backbones, and have the similar mole fraction of sodium acrylate and molecular weight, but the benzene side group in SAA–Na could decrease the interactions between molecules of SAA–Na, leading to stronger interactions between PET and SAA–Na than that of PET/AClyn. Therefore the better compatibility of PET/SAA–Na was observed.

3.2. Crystallization behaviors of PET/ionomers

The effect of ionomers on the crystallization of PET can be characterized by the cold-crystallization temperature (T_{cc}) and melt-crystallization temperature (T_{mc}) of PET samples, lower T_{cc} or higher T_{mc} corresponds to the higher crystallization rate.

Fig. 3 shows the crystallization behaviors of neat PET, A10 and S10. Evidently, the T_{mc} of PET increased greatly and the width of crystallization peak narrowed with the addition of AClyn or SAA–Na (Fig. 3(a)), and the T_{cc} also decreased considerably ((b)). All these results indicated that both AClyn and SAA–Na had high efficiency to enhance the crystallization rate of PET. Fig. 4 shows that the content of AClyn introduced as low as 0.1 wt% can enhance the T_{mc} by 11.1 °C and decrease the T_{cc} by 7.6 °C, which was better than the 0.1 wt% of SAA–Na. Increasing the content of AClyn, the T_{mc} increased and the T_{cc} decreased further, and they remained unchanged beginning with 0.5 wt% of AClyn. Similar results were obtained for the PET/SAA–Na samples. Moreover, from Fig. 4 it can be found that at the same content beyond 0.1 wt%, SAA–Na had almost the same efficiency to decrease the T_{cc} and increase the T_{mc} with AClyn.

The crystallization rate of PET can be also characterized by the half-time of crystallization ($t_{1/2}$), which is defined as the time taken from the onset of the relative crystallization until 50% completion in the isothermal crystallization process. Compared with neat PET, the $t_{1/2} \sim T_c$ curves of PET/ionomers shifted to higher temperature region at high T_c, and shifted to lower temperature region at low T_c (Fig. 5), confirming that the crystallization rate of PET was accelerated at both high and low temperature regions by the addition of AClyn or SAA–Na. Similarly in Fig. 4, the shift of temperature in the $t_{1/2} \sim T_c$ curve of PET modified by 0.1 wt% AClyn (A01) was larger than that of 0.1 wt% SAA–Na (S01) either at high or low temperature

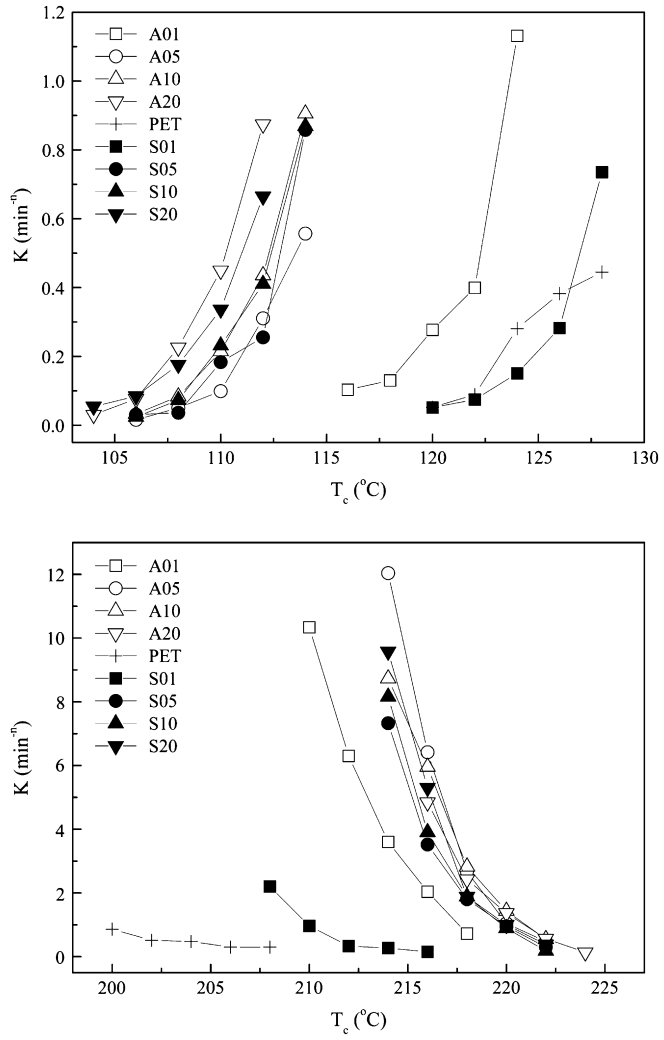

Fig. 9. Plot of crystallization rate parameter K versus the crystallization temperature (T_c) for the PET/ionomers.

region, while other PET/AClyn samples had the similar crystallization rate with PET/SAA–Na.

From previous results [8,9] and our work, it was found that AClyn or SAA–Na can survive dissolution and reaction with PET melt, and the ionomer itself acts as heterogeneous nucleating agent to enhance the crystallization rate of PET at both high and low temperature regions. Therefore, more content of ionomer results in more nucleating sites formed in PET and higher T_{mc} and lower T_{cc} were obtained, as shown in Fig. 4. Actually, PET nuclei were induced around the sodium ion aggregate of ionomer [7]. SAA–Na has less sodium ions than AClyn at the same content, then The number of nuclei of PET induced by SAA–Na should be lower than that of AClyn, and result in the less increase of crystallization rate of PET modified by SAA–Na, compared with PET modified by AClyn, which were opposite to the results showed in Fig. 5. Yu et al. [9] ascribed the higher number of heterogeneous nuclei induced by ionomer ethylene–sodium acrylate than ethylene–zinc acrylate to the better dispersion of sodium salt in PET than zinc salt. Previous discussion in this article has showed that the dispersion ability (or called compatibility) of AClyn and SAA–Na in PET was influenced by the ion–dipole interactions between PET and ionomer, which indicated that PET nuclei should be induced around the ion aggregates of ionomer through the interactions between PET and ionomer. Therefore, both the amount of sodium ions and the interactions between PET and ionomer determined the efficiency of ionomer as nucleating agent for PET. The interactions between PET and SAA–Na were stronger than that of PET/AClyn, which could lead to higher number of heterogeneous nuclei formed in PET and counterbalance the effect of fewer amounts of sodium ions in SAA–Na than AClyn. Eventually, similar nucleating efficiency was obtained for SAA–Na and AClyn.

Comparing with PET modified by 0.1 wt% of AClyn (A01), the lower crystallization rate of PET modified by 0.1 wt% of SAA–Na (S01) at both high temperature region and low temperature region (Fig. 5) can be explained by the different thermal stabilities of ionomers, as shown in Fig. 6. Below 300 °C the styrene–sodium acrylate ionomer SAA–Na lost 6.0% while the ethylene–sodium acrylate ionomer AClyn lost only 1.1%, indicating less thermal stability of SAA–Na than AClyn. Consequently, at the content of 0.1 wt%, the residue of SAA–Na is not enough to induce high number of nuclei for enhancing the crystallization rate of PET than AClyn.

3.3. Kinetic analysis

In this study, Avrami equation [26,27] was used to analyze the isothermal crystallization process of PET/ionomer:

$$1 - X_t = \exp(-Kt^n) \tag{1}$$

$$\log[-\ln(1 - X_t)] = n \log t + \log K \tag{2}$$

where X_t is the relative degree of crystallinity at time t, the exponent n is a mechanism constant with a value depending on the type of nucleation and the growth dimension, and the parameter K is a growth rate constant involving both nucleation and the growth rate parameters.

Fig. 7 shows the plots of $\log[-\ln(1 - X_t)]$ versus $\log t$ according to Eq. (2) for the isothermal melt-crystallization of neat PET, A10 and S10, other PET/ionomers had the similar results with A10 or S10. It was found that the curve for neat PET was nearly linear in the whole range of crystallization time (Fig. 7(a)). The Avrami exponent n was 2.0 ± 0.1, suggesting that the nucleation type of neat PET should be heterogeneous nucleating and its growth type should be a two-dimensional growth.

However, for the PET samples modified by AClyn or SAA–Na, all the curves were composed of two linear sections with different slopes (Fig. 7(b) and (c)). The first linear section standed for the primary crystallization process and the Avrami exponent n was about 2.2–3.5, corresponding to the growth of spherulites from heterogeneous nuclei. These results indicated that at high temperature region, the growth dimension of PET was increased by the addition of both AClyn and SAA–Na. However, it was not affected by the change of structure from AClyn to SAA–Na. The later section standed for the secondary crystallization process, which should be lower-dimensional growth, thus the Avrami exponent n was below 2.0 mostly.

All Avrami plots of both neat PET and PET/ionomers for isothermal cold-crystallization showed only one straight line. Lu et al. [28] have reported that at 118 °C for the isothermal cold-crystallization of PET, the relative degree of crystallinity at the end of the primary crystallization reached 98%, and increased with decreasing the temperature. Obviously, it's hard to detect the secondary crystallization process at lower temperature by the limited sensitivity of DSC. For this reason, there is mostly one slope for the isothermal cold-crystallization of neat PET and PET/ionomers. The Avrami exponent n had values lower than 2.0 for the majority of PET samples (Fig. 8), which corresponded to a disk-like

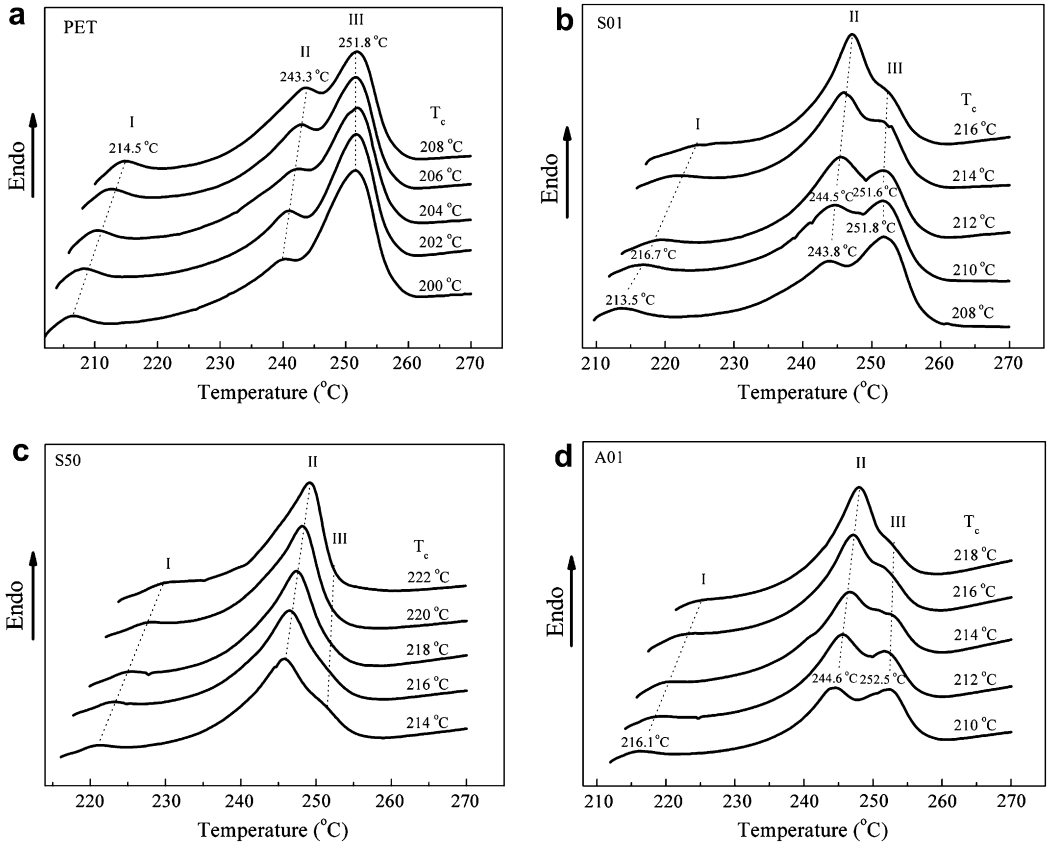

Fig. 10. Melting behaviors of (a) PET, (b) S01, (c) S50, (d) A01. Sample was heated at 10 °C/min after isothermal melt-crystallization.

morphology formed by heterogeneous nucleation [29] and indicated that the difference of structure between AClyn and SAA–Na did not change the growth dimension of PET at low temperature region.

Fig. 9 shows the effect of crystallization temperature on the crystallization rate parameter K. At high temperature region, the value of K decreased with increasing the crystallization temperature (T_c), and it increased with increasing T_c at low temperature region, which was in accordance with the tendency of $1/t_{1/2}$ (Fig. 5). At both high and low temperature regions, the K of A05 or S05 was higher than that of neat PET at the same T_c, and the K increased further with increasing the content of ionomers, indicating that more ionomer in PET could result in faster crystallization rate.

3.4. Melt behaviors of PET/ionomers

After isothermal melt-crystallization, the DSC endotherms exhibited three melting peaks for various PET samples, as shown in Fig. 10. According to the similar explanations of multiple endotherms of PET [30], peak I, which normally appeared about 10 °C above T_c, is attributed to the melting of crystals formed during secondary crystallization, peak II to the melting of the crystals formed during primary crystallization and peak III to those formed as a result of re-crystallization of peak I and peak II on heating. As the crystallization temperature (T_c) increased, more perfect crystals formed, and therefore peaks I and II were shifted to higher temperatures while peak III had little change.

Comparing the melting DSC curves of neat PET and S01 at 208 °C (Fig. 10(a) and (b)), the peak II of neat PET was 243.3 °C while that of S01 was 243.8 °C. It meant that the addition of SAA–Na increased the melting point of PET crystals formed during the primary crystallization stage. Fig. 11 presents the crystalline morphologies of various PET samples after isothermal melt-crystallization at 220 °C for 5 min. For neat PET, the size of spherulites was rather big, while for the PET modified by 0.1 wt% of SAA–Na, the size of spherulites was much smaller and uniform. As discussed previously, SAA–Na acts as heterogeneous nucleating agent to increase the crystallization rate of PET and decrease the distance between spherulites, contributing the crystals of S01 more perfect than that of neat PET and then the peak II of S01 higher than neat PET. The changes of peak III (Fig. 10(b) and (c)) at the same crystallization temperature, e.g. $T_c = 214$ °C, confirmed this further. It can be found that the peak III of S01 was observed obviously as a shoulder shape, however, the peak III of S50 was difficult to observe in its endothermal trace, indicating that the re-crystallization process on heating was reduced greatly due to more perfect crystals formed with increasing the content of SAA–Na (Fig. 11(c)). The addition of AClyn can also result in higher value of peak II and more perfect crystals, as shown in Figs. 10(d) and 11(d), respectively. Moreover, the PET modified by AClyn or SAA–Na at the same content had almost the same value of peak II.

4. Conclusions

Low molecular weight ionomers, ethylene–sodium acrylate (AClyn) and styrene–sodium acrylate (SAA–Na), were mixed with

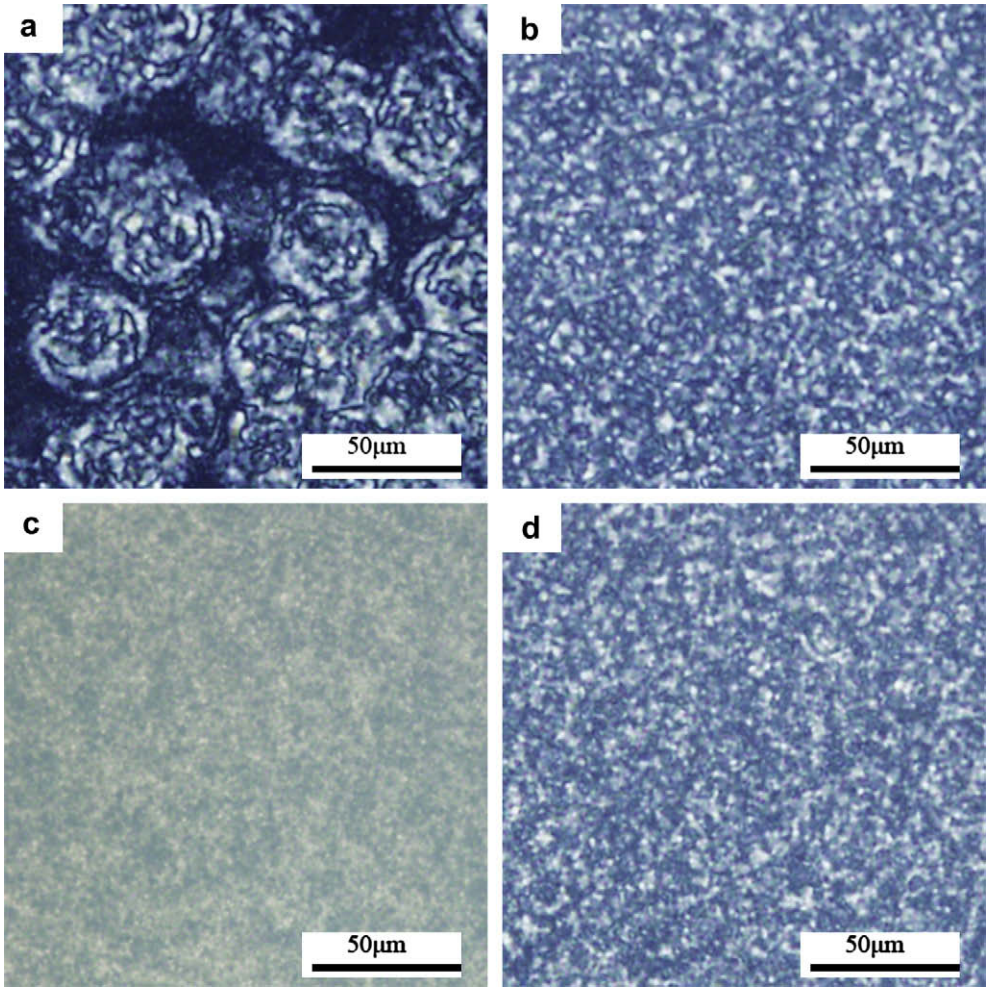

Fig. 11. POM pictures of (a) PET, (b) S01, (c) S50, (d) A01 isothermally crystallized at 220 °C for 5 min.

PET. SEM micrographs showed that voids with smooth surfaces and particles of ionomer existed in PET/AClyn, however, in PET/SAA–Na, only particles strongly bonded to the PET matrix because of the presence of benzene group in SAA–Na.

During crystallization, SAA–Na and AClyn acted as heterogeneous nucleating agents at both high and low temperature regions. At the same content beyond 0.1 wt%, PET/SAA–Na showed similar crystallization rate with PET/AClyn. Kinetic analysis showed that the Avrami exponent *n* was not influenced by the structural difference between AClyn and SAA–Na. For isothermal melt-crystallization, it was about 2.2–3.5, while for isothermal cold-crystallization it was close to 2.0.

After isothermal melt-crystallization, multiple melting endotherms were obtained for all PET/ionomer samples in the subsequent DSC heating scan, but the second melting peak of PET/AClyn or PET/SAA–Na was higher than that of PET due to the formation of more perfect crystals.

References

[1] Groeninekx G, Berghmans H, Overbergh N, Smets G. J Polym Sci Polym Phys Ed 1974;12:303–16.
[2] Run MT, Wu SZ, Zhang DY, Wu G. Polymer 2005;46:5308–16.
[3] Ke YC, Wu TB, Xia YF. Polymer 2007;48:3324–36.
[4] Legras R, Bailly C, Daumeie M, Dekoninck JM, Mercier JP. Polymer 1984;25:835–44.
[5] Garcia D. J Polym Sci Polym Phys Ed 1984;22:2063–72.
[6] Gilmer JW, Neu RP, Liu YJ, Jen AKY. Polym Eng Sci 1995;35:1407–12.
[7] Scheirs J. Additives for the modification of poly(ethylene terephthalate) to produce engineering-guide polymers. In: Scheirs J, Long TE, editors. Modern polyesters. New York: John Wiley & Sons Ltd; 2003. p. 515–20.
[8] Yu Y, Yu YL, Jin MN, Bu HS. Macromol Chem Phys 2000;201:1894–900.
[9] Yu Y, Bu HS. Macromol Chem Phys 2001;202:421–5.
[10] Ronald RL. US Patent, Reinforced polyester molding compositions, 4803237; Feb 22 1988.
[11] Ronald RL. US Patent, Injection molding glass fiber reinforced polyester with improved surface finishes, 4810744; Apr 4 1988.
[12] Edward JD. GB Patent, Molding resins, 2015014; Jan 5 1979.
[13] Murali KA, Bruce VanBuskirk, Sengshiu JC. US Patent, Polyester molding compositions and articles exhibiting good impact, heat and solvent resistance, 5723520; Aug 9 1996.
[14] Nield E, Higgins DE, Young MW. US Patent, Fast crystallizing polyester compositions, 4380621; Nov 28 1980.
[15] Ramesan MT, Lee DS. Iran Polym J 2008;17:281–8.
[16] Kalfoglou NK, Skafidas DS, Sotiropoulou DD. Polymer 1994;35(17):3624–30.
[17] Iyer S, Schiraldi DA. J Polym Sci Part B Polym Phys 2006;44:2091–103.
[18] Guerrero C, Lozano T, González V, Arroyo E. J Appl Polym Sci 2001;82:1382–90.
[19] Mascia L, Bellahaeb F. Adv Polym Technol 1994;13(2):99–109.
[20] Retolaza A, Eguiazábal JI, Nazábal J. J Appl Polym Sci 2003;87:1322–8.
[21] Retolaza A, Eguiazábal JI, Nazábal J. Polym Eng Sci 2002;42(11):2072–83.
[22] Świtata M, Wojtczak Z. Makromol Chem 1986;187:2411–8.
[23] Daaneels DF. J Plast Film Sheeting 1988;4:250.
[24] Park HD, Park KO, Cho WJ, Ha CS, Kwon SK. Polym Recyl 1996;2:283–9.
[25] Suchocka-Gałas K. J Appl Polym Sci 2003;89:55–62.
[26] Avrami M. J Chem Phys 1939;7:1103–12.
[27] Avrami M. J Chem Phys 1940;8:212–24.
[28] Lu XF, Hay JN. Polymer 2001;42:9423–31.
[29] Wellen RMR, Rabello MS. J Mater Sci 2005;40:6099–104.
[30] Kong Y, Hay JN. Polymer 2003;44:623–33.